

Fragment Docking to S100 Proteins Reveals a Wide Diversity of Weak Interaction Sites

Yvonne Arendt,^[d] Anusarka Bhaumik,^[a] Rebecca Del Conte,^[a, d]
 Claudio Luchinat,^{*,[a, b, c]} Mattia Mori,^[a, d] and Marco Porcu^[a]

The S100 protein family is a highly conserved group of Ca²⁺-binding proteins that belong to the EF-hand type and are considered potential drug targets. In the present study we focused our attention on two members of the family: S100A13 and S100B; the former is involved in the nonclassical protein release of two proangiogenic polypeptides FGF-1 and IL-1 α that are involved in inflammatory processes, whereas S100B is known to interact with the C-terminal domain of the intracellular tumor suppressor p53 and promote cancer development. We screened, using waterLOG-SY NMR experiments, 430 molecules of a generic fragment library

and we identified different hits for each protein. The subset of fragments interacting with S100B has very few members in common with the subset interacting with S100A13. From the ¹⁵N-HSQC NMR spectra of the proteins in the presence of those hits the chemical shift differences $\Delta\delta(\text{HN})$ were calculated, and the main regions of surface interaction were identified. A relatively large variety of interaction regions for various ligands were identified for the two proteins, including known or suggested protein–protein interaction sites.

Introduction

S100 proteins are low-molecular weight protein dimers. Each monomer is constituted by an EF-hand domain, a domain containing two helix-loop-helix motifs interconnected by a linker (hinge loop for S100) and capable of binding two calcium ions in the loops in a characteristic way. The canonical loop is 12 aa long. The EF-hand domain in S100 proteins is characterized by the first loop being noncanonical (14 aa long) and by the first and last helices preceded and followed by residues with no secondary structure.^[1] Twenty members have been identified so far in the human genome and, altogether, S100 proteins represent the largest family in the human calcium-binding EF-hand protein superfamily. These proteins are only found in vertebrates, and different members of the family are expressed in a tissue-specific and cell type-specific pattern. S100 genes are expressed in many tissues including those of the nervous system, musculature, skin, adipose tissues, reproductive system, gastrointestinal system, respiratory system, and urinary system.^[2–4] Importantly, these proteins regulate intracellular processes such as cell growth and mobility, cell cycle regulation, transcription, and differentiation.^[3,5–7] This suggests that different S100s have different functions, and as they do not have any catalytic activity of their own it is likely that they regulate the activity of other proteins.^[8] Many of these regulatory pathways involve a direct interaction of a specific S100 protein with a particular target protein, so it is reasonable to expect that different members of the S100 family have quite different physiological roles. Misregulation of any of these interactions can thus cause pathologies, which makes S100 proteins potential drug targets.

It is widely appreciated that inhibiting protein–protein interactions is a more difficult goal than inhibiting, for example, en-

zymatic functions,^[9,10] and this is the reason why drug discovery programs have not made much progress in this area. For example, the well-known family of matrix metalloproteinases (MMP) are enzymes with a well-defined catalytic role, whereas S100 are in general modulators of different protein activities, so the interaction site is very well defined in MMPs and as yet largely undefined in S100 proteins. However, MMPs suffer from the problem that they have very similar structures and functions, and inhibiting a particular MMP selectively without affecting the other members of the family is difficult.^[11,12] Conversely, the S100 protein family members have a variety of partners and therefore it may be hoped that selectivity is more easily achieved. Therefore in this study we decided to look at

[a] A. Bhaumik, R. Del Conte, C. Luchinat, M. Mori, M. Porcu
 Magnetic Resonance Center (CERM)
 University of Florence
 via Luigi Sacconi, 6, 50019 Sesto Fiorentino (FI) (Italy)
 Fax: (+39)055-4574271
 E-mail: luchinat@cerm.unifi.it

[b] C. Luchinat
 Department of Agricultural Biotechnology
 University of Florence
 Via Maragliano, 75-77-50144 Firenze (FI) (Italy)

[c] C. Luchinat
 FIORGEN Fondazione Farmacogenomica
 Polo Scientifico
 via Luigi Sacconi, 6-50019 Sesto Fiorentino (FI) (Italy)

[d] Y. Arendt, R. Del Conte, M. Mori
 ProtEra S.r.l.
 University Scientific Campus
 viale delle Idee, 22, 50019 Sesto Fiorentino (FI) (Italy)

Supporting information for this article is available on the WWW under <http://www.chemmedchem.org> or from the author.

two different S100 proteins (S100B and S100A13) to 1) explore their whole surface for possible docking positions and 2) check how analogous or different the patterns of the ligand binding sites are for the two proteins. S100B is reported to interact with the C-terminal peptide of p53,^[13–16] and to be involved in cancer through the regulation of the p53 protein,^[17–21] a known tumor suppressor factor. Moreover, for the S100B–p53 interaction, it was found that phosphorylation of specific serine and/or threonine residues reduces the affinity of the S100B–p53 interaction by as much as an order of magnitude, and is important for protecting p53 from S100B-dependent downregulation.^[22] S100A13 has been recently designated as a new marker of angiogenesis in human astrocytic gliomas,^[23] and as a regulator of the FGF-1 release.^[24–26] NMR is one of several techniques to support drug discovery efforts.^[27–29] NMR screening is especially appreciated for its robustness in not producing false positive results, and for its sensitivity to identify weak interactions.^[30–32] In the present work both S100 proteins were screened by NMR towards a fragment library (430 members). We found that a large variety of weak-binding sites in the two proteins (low mM–high μ M range) exist, with little overlap between the fragments that bind to one or the other protein. We have also found that in the case of S100B there are two main sites that are able to bind fragments of the library and are potentially overlapping with the interaction area of the p53 C-terminal peptide. Interestingly, S100A13 does not show appreciable affinity for these ligands, confirming our hypothesis that the variety of functions of S100 proteins may make it easier to find selective ligands for individual members of this family. This is a further step to attempt drug design strategies for these proteins.

Results and Discussion

NMR-based screening and mapping of the binding sites

An NMR based screening was conducted using the ligand-based waterLOGSY (water-ligand observed by gradient spectroscopy) technique on calcium-loaded S100A13 and S100B.^[33] The fragment library of ProtEra S.r.l. was used, containing 430 commercially available fragments as chemically diverse as possible (see Table 1 and Figure 1). The library is small and generic, and was purposely built to also contain smaller than usual fragments. From waterLOGSY experiments 56 and 47 frag-

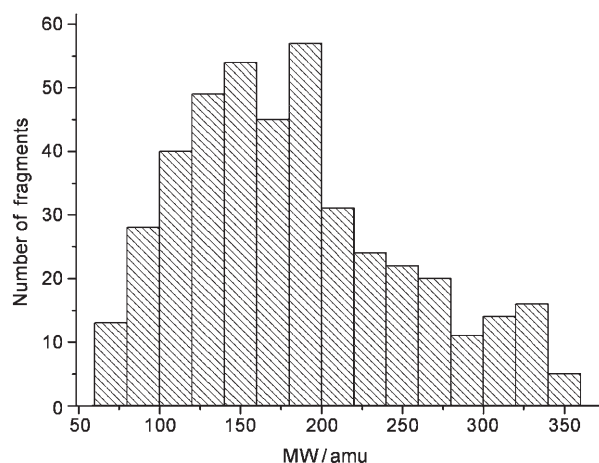


Figure 1. Molecular weight distribution of the fragment library.

ments showed an interaction with S100A13 and S100B, respectively. Only 13 fragments bind both proteins.

The interaction mode of the fragments having significant effect in waterLOGSY, as well as of the antiallergic drug cromolyn, known to interact with S100A13,^[34,35] were categorized on the basis of their scaffold similarity, into 17 groups. Fragments belonging to the same group present similar chemical shift variation patterns. For each group at least one fragment was further investigated by following the titration of the proteins with the selected fragments through ¹⁵N-HSQC spectra. The chemical shift perturbation ($\Delta\delta(\text{NH})$ or Garrett values), of uniformly ¹⁵N-labeled protein samples upon complex formation with a ligand provides a sensitive tool for the identification of binding sites. The ¹⁵N and ¹H backbone resonances in the ligand–protein complexes were assigned by following the previously assigned cross peaks in the ¹⁵N-HSQC spectrum of each S100 protein alone. The fragments of each group determine similar distributions of the chemical shift perturbation.

The interacting fragments and the areas of interaction with S100B and S100A13, with significant ¹⁵N-HSQC spectra perturbations ($\Delta\delta(\text{NH}) > 0.03$ ppm), are reported in Table 1S of the Supporting Information. A relatively small fraction of the compounds in Table 1S have a molecular weight smaller than 150, which is empirically considered to be a lower limit for “ideality” of a hit. For the present purposes, these less than ideal hits still provide useful information. Figures 2 and 3 represent the chemical shift variation of S100B and S100A13 while interacting with the ligand 1-naphtol (5B) and the antiallergic drug cromolyn respectively.

A detailed analysis of Table 1S reveals that there are two main binding areas for ligands on S100B. The first area involves the hinge loop and the C-terminal part of helix α_4 , the second area involves the hinge loop and helix α_3 (Figure 4). On the other hand, in the case of S100A13 three main binding areas can be identified, that is: 1) the second calcium binding site with the C-terminal part of helix α_1 ; 2) the hinge loop region between helix α_2 and helix α_3 , which extends to the C-terminal part of helix α_4 and the N-terminal part of helix α_1 of the second subunit; 3) the interaction area between the two sub-

Table 1. Characteristics of the fragment library.

	Min. value	Max. value	Average value
Molecular Weight	68	350	181.9
Number of HEAVY atoms	2	26	12.5
Number of rings	0	5	1.4
Ring size	3	7	5.8
LogP	−2.5	8.8	1.1
ClogP	−9.2	6.1	0.9
H-bond donors	0	5	1.3
H-bond acceptors	0	6	2.5

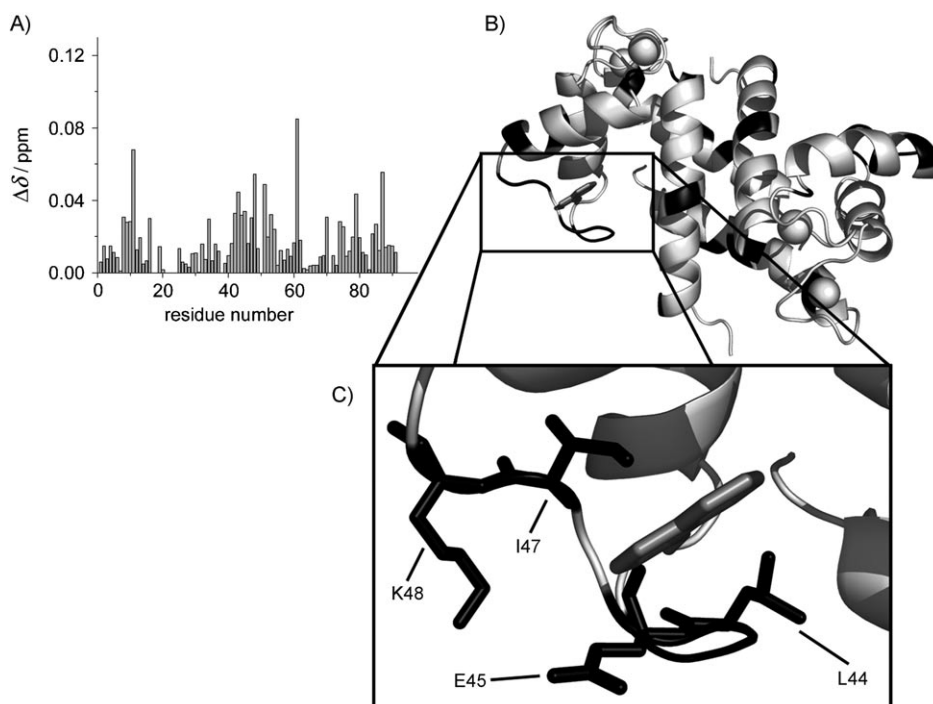


Figure 2. A) Plot of the chemical shift variations (Garrett values) for the S100B-5B adduct. B) Residues showing significant chemical shift variations ($\Delta\delta > 0.03$ ppm) are reported in black for both the protein subunits. C) Detail of the S100B-1-naphtol interaction: in black sticks are represented the residues with non-negligible chemical shift closest to the ligand.

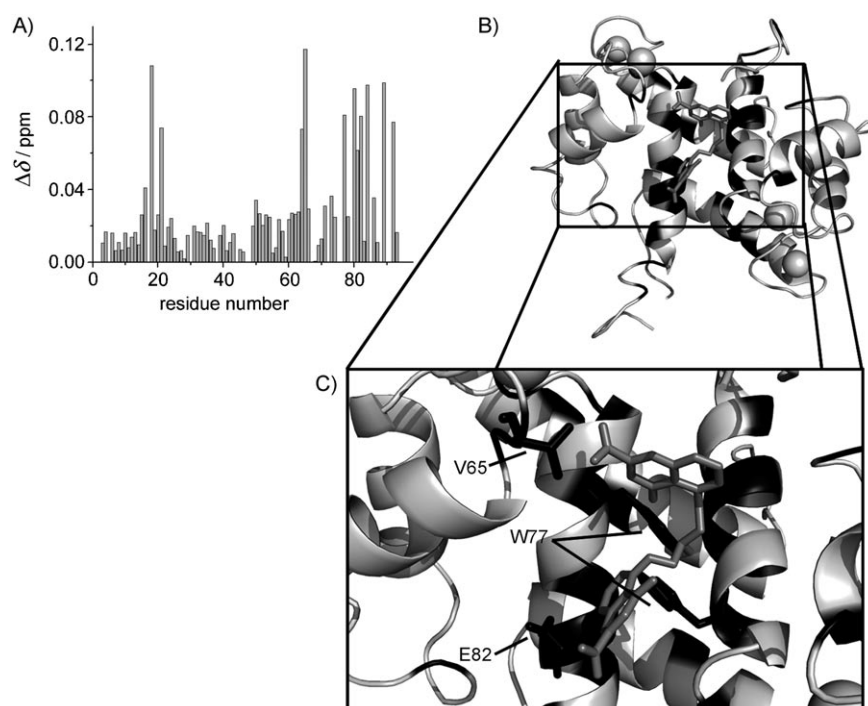


Figure 3. A) Plot of the chemical shift variations (Garrett values) for the S100A13-cromolyn adduct. B) Residues showing significant chemical shift variations ($\Delta\delta > 0.03$ ppm) are reported in black for both the protein subunits. C) Detail of the S100A13-cromolyn interaction: in black sticks are represented the residues with non-negligible chemical shift, closest to the ligand.

units, which could involve helix α_4 and/or helix α_1 (Figure 5). For the ligands showing the largest effects in the waterLOGSY

usually, taking into account both the agreement with the NMR data and the free-binding energy of the ligand–protein com-

and HSQC experiments, K_d values were calculated from chemical titrations and reported in Table 2. From the knowledge of the K_d we calculated the ligand efficiency (LE) of each fragment, defined as:

$$LE = -\Delta G / N_{\text{nonhydrogen atoms}} \quad (1)$$

$$\approx -RT \ln(K_d) / N_{\text{nonhydrogen atoms}}$$

The concept of ligand efficiency, introduced by the pioneering work of Kuntz, Kollman, and colleagues, can be used to assess the quality of initial screening hits and also the quality of the leads as they are optimized,^[36–38] LE values higher than 0.3 are considered a good starting point for the hit-to-lead development process. Our results showed that two ligands for S100B and three ligands for S100A13, have LE values higher than 0.3 (Table 2). These ligands should then be a good starting point to develop protein ligands with high drugability potential.

To identify the binding conformation of the hits, we coupled the experimental NMR data with docking calculations, using the AutoDock program, as recently reported by K. A. Mercier and colleagues.^[39]

S100A13

Docking: Docking calculations were carried out to identify the more probable binding conformations for each of the 24 ligands with non-negligible chemical shift variations ($\Delta\delta > 0.03$ ppm, Table 1S).

The docking calculations were performed on three different potential grid maps, covering the entire protein volume, centered on the three binding areas identified by the NMR screening (the docking protocol is described in the experimental section). The analyses were performed man-

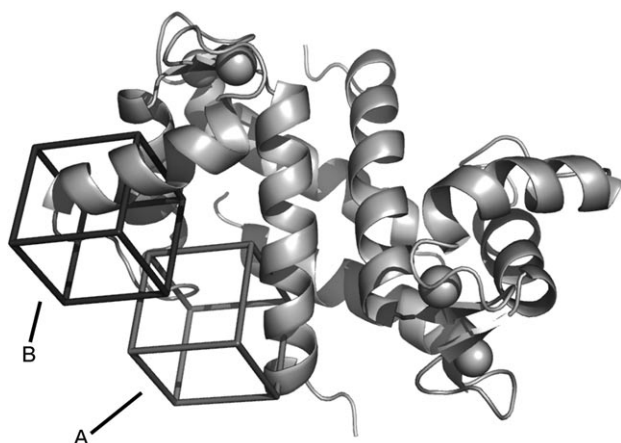


Figure 4. Structure of S100B. Box A (in light gray) contains the binding area involving the hinge loop and the C-terminal part of helix $\alpha 4$. Box B (in dark gray) contains the binding area involving the hinge loop and helices $\alpha 3$ and $\alpha 4$. The calcium ions are shown (two for each subunit) as spheres.

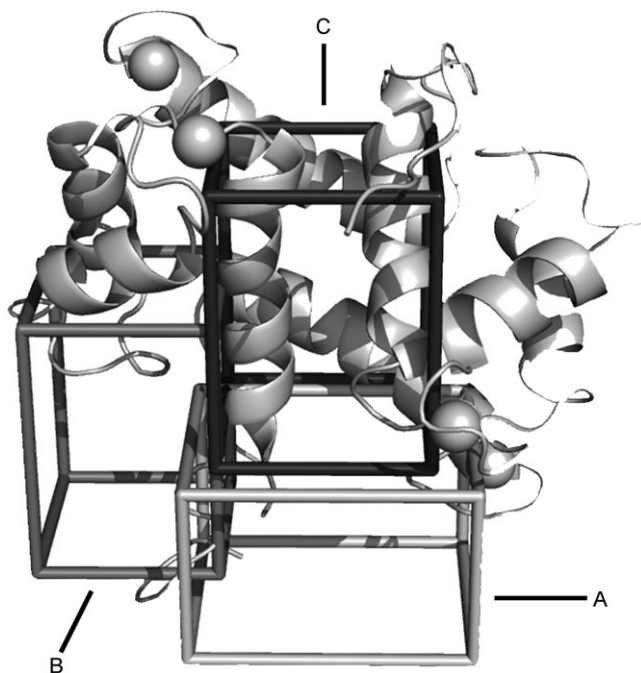


Figure 5. Structure of S100A13. Box A (in light gray) contains the binding area involving the second calcium binding site and the C-terminal part of helix $\alpha 1$; Box B (in gray) contains the binding area involving the hinge loop region between helix $\alpha 2$ and helix $\alpha 3$, the C-terminal part of helix $\alpha 4$ and the N-terminal part of helix $\alpha 1$ of the second subunit; Box C (in dark gray) contains the binding area involving helices $\alpha 4$ at the interface between the two subunits.

plex provided by the docking results. The docking results are consistent with the presence of three main binding areas on the protein S100A13. In particular the compounds warfarin (21M), anthraquinone-sulfonic acid (3S), 2,6-naphthalenedisulfonic acid (11B), 3,5-pyrazoledicarboxylic acid (11L), benzo-thiophene (12Z), and furosemide (17K) preferentially interact in area 1, the compound 2,3-dicarboxypyridine (9A) preferentially

interacts in area 2, and the compounds bisphenol A (4E), cimetidine (17C), (L)-glutamic acid (13Y) preferentially interact in area 3. For each of the ligands we found at least one cluster of docking conformations in agreement with the area identified by the NMR experiments.

Cromolyn binding. In 1997 and 1999 Kobayashi et al. demonstrated that three different antiallergic drugs, including cromolyn, bind to S100A13.^[40,41] To investigate the molecular basis of this interaction, we performed a ^{15}N -HSQC titration of S100A13 with cromolyn. Plots of $\delta\Delta(\text{HN})$ versus ligand concentration for the most shifted residues (T18, F21, V65, A84, and K89) give a good fitting with the one binding site equation ($R^2 \approx 0.97$). Docking calculations generated two clusters of conformations, in agreement with the experimental data, binding in areas A and C of Figure 5; however the cluster interacting near the helices $\alpha 4$ (area C of Figure 5) is characterized by a final docked energy thirty percent lower with respect to the others; in this solution cromolyn is close to many of the residues with high chemical shift variation, in particular V65 of loop III and W77 and E82 of helix $\alpha 4$ (Figure 3C). Our data thus provide a structural basis for this interaction.

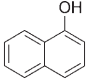
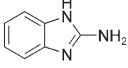
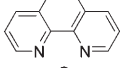
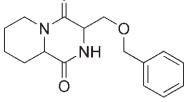
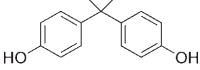
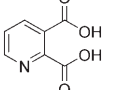
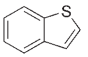
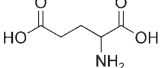
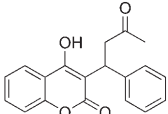
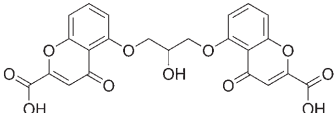
S100B

Docking. All the fragments interacting with S100B by water-LOGSY experiments were docked on the surface of the S100B protein and, as for S100A13, the docking solutions were analyzed manually, according to the agreement between the HSQC data and the free-binding energy of the ligand–protein complex. Two possible interaction areas have been identified, located around the hinge loop. In particular, the first one is characterized by the pocket involving the hinge loop, helix $\alpha 1$ and mostly the C-terminal portion of helix $\alpha 4$ (F87, C84, F43, L44, and V8) (see Figure 3A). The compounds (L)-tryptophan-methylester (16G), 1,10-phenantroline (2T), and (3R,9R)-3-((benzyloxy)methyl)-hexahydro-6H-pyrido[1,2]pyrazine-1,4-dione (AC) preferentially interact in this surface region, justifying the chemical shift variations observed especially in the first part of helix $\alpha 1$. The second interacting area also involves the hinge loop and the helix $\alpha 3$ in its N-terminal part. The compounds showing significant interactions in the second area are 1-naphthol (5B), 2-aminobenzimidazole (19V) and (3R,9R)-3-((benzyloxy)methyl)-hexahydro-6H-pyrido[1,2]pyrazine-1,4-dione (AC). These interactions are responsible for the largest chemical shift variations observed in helix $\alpha 2$ and helix $\alpha 3$.

Analysis of the docking results reveals that most of the fragments bind exclusively in one of the two areas identified. In a fragment based approach the identified fragments binding in different areas should be subsequently linked with the intent to obtain stronger interacting compounds for S100B.

Competition with P53. To check the potential of fragment 5B (1-naphthol), interacting with the p53 binding region of S100B, ^{15}N -HSQC titration was performed in the presence of a peptide known to interact with S100B, derived from the C-terminal regulatory domain of p53. Compound 5B was chosen because it has the lowest K_d value observed for the interacting fragments. The p53 peptide affects several peaks (especially in

Table 2. K_d and ligand efficiency (LE) values calculated for interesting hits for S100A13 and S100B.

Molecular formula	Library code	K_d [mM] on S100A13	K_d [mM] on S100B	Residues with $\Delta\delta(\text{NH}) > 0.03$ ppm
	5B	–	~ 0.1 LE = 0.50	8,11,16,42,43,45, 47,48,51,53,61,70,79,87
	19V	–	~ 1.5 LE = 0.38	4,5,9-12,25,43,59, 75,77,79,82, 84-89
	2T	–	~ 2.3 LE = 0.26	1,4,8,9,11,16,18, 41-43,54,55,58, 61,75,80,82,84, 88-90
	AC	–	~ 1.0 LE = 0.20	8,-10,19,35,37,42, 43,48,62,71,73,75,76,79-81,83-85, 87-91
	4E	~ 0.9 LE = 0.24	–	49, 50, 52, 53, 54, 82
	9A	~ 0.9 LE = 0.35	–	2, 6-8, 11, 12, 14, 18, 24, 25, 34, 38, 43, 49, 56, 65, 73, 74, 77, 78, 81, 85, 87, 89
	12Z	~ 1.8 LE = 0.42	–	7, 8, 11, 12, 14, 18, 24, 25, 30, 34, 40, 64, 65, 78, 80 –82, 84, 89
	13Y	~ 2.3 LE = 0.43	–	4, 7, 8, 11, 12, 14, 18, 24-26, 34, 43, 48, 50, 83, 86, 87, 89, 92,
	21M	~ 0.7 LE = 0.19	–	6, 11 18, 20, 22, 71, 73, 74,77, 78, 81-84, 86, 89, 93
	cromolyn	~ 0.3 LE = 0.14	–	16, 18, 21, 50, 64, 65, 71 73, 77, 80, 81, 82, 84, 86, 89, 92

helix $\alpha 1$, the hinge region, helix $\alpha 3$, helix $\alpha 4$, and the C-terminal region) in a ^{15}N -HSQC titration on the protein; 5B alone affects several peaks already described, some of which are in common with p53 peptide. ^{15}N labeled S100B was first titrated with p53 peptide up to a 1:2 molar ratio with respect to the S100B monomer, and 5B was added stepwise up to a molar ratio of 1:2:4, respectively. Further addition of 5B resulted in the precipitation of the protein. Comparing the four spectra of 1) S100B:5B; 1:2; 2) S100B:p53 peptide; 1:2; 3) S100B:p53 peptide: 5B; 1:2:2; 4) S100B:p53 peptide:5B; 1:2:4, we observed that the addition of the 5B fragment to the S100B–p53 peptide complex has different effects on different peaks. Several of them are restored to the original position in the S100B–5B adduct (see Figure 6 A and B). Most of these peaks are located on helix $\alpha 3$, in the proximity of the hinge loop (Q51, V52, V53, D54, K55, V56, M57). Some other peaks were shifted to a new position (L10, H15, G19, S30, E31, E34, N38, S62, D63, G66, E67, D69, F73, M74, F88) different from their original positions in S100B–5B and S100B–p53 peptide adducts. This points to 5B replacing a portion of the bound peptide molecule, with a mixed competitive/noncompetitive behavior. The other portion

of the peptide presumably rearranges in a new conformation to avoid conflict with the surface portion occupied by 5B. The peaks that are restored clearly identify the region of the protein where 5B binds, displacing a portion of the peptide.

Conclusions

Two S100 proteins with a potential to become drug targets were screened by NMR with a library of 430 fragments. The results of this study allowed us to identify three main binding areas for S100A13 and two main binding areas for S100B. This result is somewhat surprising, as small proteins usually display only one major binding site for small molecules.^[42] Incidentally, none of the binding areas suggest binding of ligands to calcium ions. Although the two proteins have quite similar quaternary structure and a common binding area (around the hinge loop), our results showed that they have only a few ligands in common, suggesting that selective leads could be developed starting from the different ligands with high LE values, identified herein. These data also indicate that the present library, although small, is well suited to make initial guesses about se-

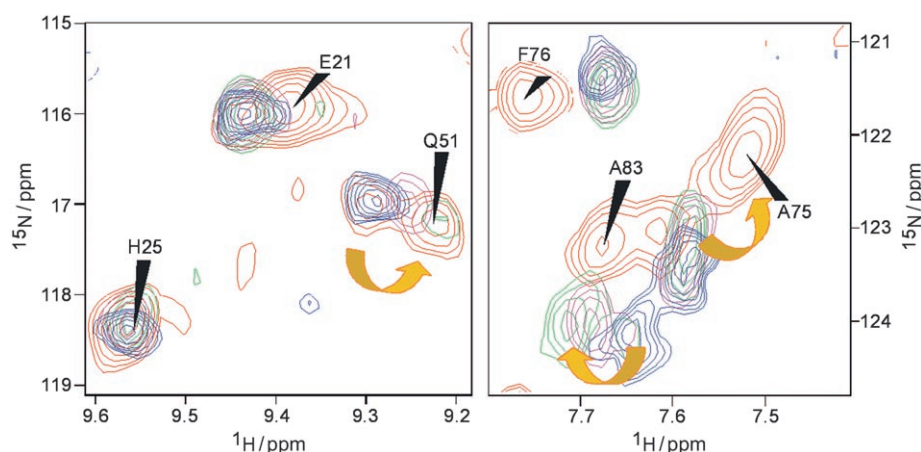


Figure 6. Superimposition of two areas of ^{15}N -HSQC spectra of 1) S100B + 5B adduct at 1:2 ratio (red); 2) S100B + p53 at 1:2 (blue); 3) S100B + p53 + 5B at 1:2:2 (magenta); 4) S100B + p53 + 5B at 1:2:4, (green).

lectivity. Essentially the same library had been used in a screening work on cytochrome c.^[43] In that case, the hits were fewer, and again the overlap with the present hits was very small. These statistics are summarized in Figure 1S. Coupling of the experimental data with docking results indicated the most probable docked conformations of the ligands on the proteins surface. The study on the antiallergic drug cromolyn provided for the first time structural information for the interaction, and demonstrated that cromolyn has a unique binding site on the protein surface. Finally, competition experiments conducted with α -naphthol on the S100B–p53 peptide complex showed that even if the ligands identified by the NMR screening bind weakly on the protein surface, they are able to significantly interfere with the interaction with other proteins or peptides. These results could be a starting point for the development of new ligands which could have an important role in the protection of p53 from S100B-dependent downregulation. S100 proteins in general are becoming targets of pharmaceutical interest because of their involvement in cellular functions. The present data suggest that selective and high efficacy modulators of their activity are within reach of current lead development strategies.

Experimental Section

Protein preparation: Human S100A13 and bovine S100B were expressed and purified as previously reported to obtain unlabeled and ^{15}N labeled proteins.^[44,45]

NMR-based screening: For all the NMR experiments S100A13 samples were prepared in acetate buffer 20 mM pH 5.6, and S100B samples were prepared in HEPES buffer 30 mM pH 6.5 plus KCl 50 mM. Samples for waterLOGSY experiments were prepared at a monomeric concentration of 20 μM of both S100A13 and S100B, and with candidate ligand concentrations of 800 μM . Samples for ^{15}N -HSQC spectra were prepared at a monomeric protein concentration of 100 μM and 400 μM for S100A13 and S100B, respectively. All NMR experiments were performed at 298 K on a Bruker Avance 700 spectrometer equipped with a sample changer, and on Avance 800 and 900 spectrometers both equipped with cryoprobes. NMR-based screening was conducted using WaterLOGSY spectra as the

primary method of screening. For each compound, a reference 1D spectrum of the compound alone and a 1D WaterLOGSY spectrum in the presence of the protein were recorded. WaterLOGSY NMR experiments employed a 2 ms selective rectangular 180° pulse at the water signal frequency and a NOE mixing time of 2 s. To map the interacting surface of the proteins, titration of the fragments were followed through ^{15}N -HSQC spectra. K_d values were calculated by plotting the weighted average ^1H and ^{15}N chemical shifts of selected residues as a function of fragment concentration added during the titration considering the one site binding mode. Garrett values are given by equation^[46]

$$\Delta\delta(\text{NH}) = \sqrt{\frac{[\Delta\delta(^1\text{H})]^2 + [\Delta\delta(^{15}\text{N})/5]^2}{2}} \quad (2)$$

Docking: Docking calculations were performed on a Open Motics cluster equipped with nine AMD Athlon 3.0 GHz processors running Gentoo Linux. The molecules were manipulated using ChemOffice Pro version 8.0. The atomic partial charges of the fragments were calculated using the semiempirical MNDO/3 and PM3 methods implemented in the Chem3D 8.0 program, whereas for the proteins S100A13 (PDB code: 1YUU) and S100B (PDB code: 1DT7) we assigned the atom types and the charges using AMBER force field. With the program AutoGrid we generated three grids of size $70 \times 70 \times 70 \text{ \AA}$ and with a grid spacing of 0.375 \AA (three for S100A13 and one for S100B). The grid boxes was centered respectively: on the helix- $\alpha 1$, near the calcium (S100A13 GRID 1), on the two tryptophans 77 of the helix- $\alpha 4$, at the interface between the two monomers (S100A13 GRID 2), on the hinge-loop (S100A13 GRID 3), and in the hydrophobic cluster between helices $\alpha 3$ and $\alpha 4$ and hinge loop, close to the side chain of I47 (S100B GRID). The ligands were docked with the program AutoDock (version 3.05). For each docking experiment we performed a global search using the Lamarckian genetic algorithm (LGA) to find the possible areas of minimum energy of interaction and a local search (LS) to optimize the energy and to search for the best conformers. During the docking process, a maximum of 100 conformers was considered for each compound (the default is ten conformers). The initial position of each ligand was on the center of the box and oriented randomly. The initial population was constituted by 100 random individuals. Step sizes of 0.2 \AA for translation and 5° for rotation were chosen and a maximum number of 1 500 000 energy evaluations and 28 000 generations was considered. Operator weights for crossover, mutation, and elitism were default parameters (0.80, 0.02, and 1, respectively). The AutoDock scoring function was used and the first four clusters of solutions were furthermore analyzed one by one to check the agreement between the docking position on the surface and the experimental screening results.

Acknowledgements

This work was supported by Ente Cassa di Risparmio di Firenze, Fondazione Monte dei Paschi di Siena, and the EC contracts:

Marie Curie-TOK contract n. MTKI-CT-2004-509750, Nano4Drugs contract n. LSHB-CT-2005-019102, NDDP contract n. LSHG-CT-2004-512077. We thank Prof. Ivano Bertini for discussions and critical reading of the manuscript, Dr. Andrea Giachetti for helpful discussions on docking calculations, and Dr. Elisa Bettazzi for help in the preparation of library samples.

Keywords: drug design • NMR spectroscopy • S100 • screening fragments • waterLOGSY

- [1] R. Donato, *Microsc. Res. Tech.* **2003**, *60*, 540–551.
- [2] R. J. Allore, W. C. Friend, D. O'Hanlon, K. M. Neilson, R. Baumal, R. J. Dunn, A. Marks, *J. Biol. Chem.* **1990**, *265*, 15537–15543.
- [3] D. B. Zimmer, E. H. Cornwall, A. Landar, W. Song, *Brain Res. Bull.* **1995**, *37*, 417–429.
- [4] K. Ridinger, B. W. Schafer, I. Durussel, J. A. Cox, C. W. Heizmann, *J. Biol. Chem.* **2000**, *275*, 8686–8694.
- [5] R. Donato, *Biochim. Biophys. Acta Mol. Cell Res.* **1999**, *1450*, 191–231.
- [6] R. Donato, *Int. J. Biochem. Cell Biol.* **2001**, *33*, 637–668.
- [7] B. W. Schafer, C. W. Heizmann, *Trends Biochem. Sci.* **1996**, *21*, 134–140.
- [8] D. B. Zimmer, S. P. Wright, D. J. Weber, *Microsc. Res. Tech.* **2003**, *60*, 552–559.
- [9] M. Martinell, X. Salvatella, J. Fernandez-Carneado, S. Gordo, M. Feliz, M. Menendez, E. Giral, *ChemBioChem* **2006**, *7*, 1105–1113.
- [10] J. Y. Trosset, C. Dalvit, S. Knapp, M. Fasolini, M. Veronesi, S. Mantegani, L. M. Gianellini, C. Catana, M. Sundstrom, P. F. Stouten, J. K. Moll, *Proteins Struct. Funct. Bioinf.* **2006**, *64*, 60–67.
- [11] P. Cuniasse, L. Devel, A. Makaritis, F. Beau, D. Georgiadis, M. Matziari, A. Yiotakis, V. Dive, *Biochimie* **2005**, *87*, 393–402.
- [12] S. L. Johnson, M. Pellecchia, *Curr. Top. Med. Chem.* **2006**, *6*, 317–329.
- [13] C. Delphin, M. Ronjat, J. C. Deloulme, G. Garin, L. Debussche, Y. Higashimoto, K. Sakaguchi, J. Baudier, *J. Biol. Chem.* **1999**, *274*, 10539–10544.
- [14] R. R. Rustandi, A. C. Drohat, D. M. Baldisseri, P. T. Wilder, D. J. Weber, *Biochemistry* **1998**, *37*, 1951–1960.
- [15] R. R. Rustandi, D. M. Baldisseri, A. C. Drohat, D. J. Weber, *Protein Sci.* **1999**, *8*, 1743–1751.
- [16] R. R. Rustandi, D. M. Baldisseri, D. J. Weber, *Nat. Struct. Biol.* **2000**, *7*, 570–574.
- [17] M. R. Fernandez-Fernandez, D. B. Veprintsev, A. R. Fersht, *Proc. Natl. Acad. Sci. USA* **2005**, *102*, 4735–4740.
- [18] J. Lin, M. Blake, C. Tang, D. Zimmer, R. R. Rustandi, D. J. Weber, F. Carrier, *J. Biol. Chem.* **2001**, *276*, 35037–35041.
- [19] J. Lin, Q. Yang, Z. Yan, J. Markowitz, P. T. Wilder, F. Carrier, D. J. Weber, *J. Biol. Chem.* **2004**, *279*, 34071–34077.
- [20] C. Scotto, J. C. Deloulme, D. Rousseau, E. Chambaz, J. Baudier, *Mol. Cell. Biol.* **1998**, *18*, 4272–4281.
- [21] C. Scotto, C. Delphin, J. C. Deloulme, J. Baudier, *Mol. Cell. Biol.* **1999**, *19*, 7168–7180.
- [22] P. T. Wilder, J. Lin, C. L. Bair, T. H. Charpentier, D. Yang, M. Liriano, K. M. Varney, A. Lee, A. B. Oppenheim, S. Adhya, F. Carrier, D. J. Weber, *Biochim. Biophys. Acta Mol. Cell Res.* **2006**, *1763*, 1284–1297.
- [23] M. Landriscina, G. Schinzari, L. G. Di, M. Quirino, A. Cassano, E. D'Argento, L. Lauriola, M. Scerrati, I. Prudovsky, C. Barone, *J. Neuro-Oncol.* **2006**, *80*, 251–259.
- [24] I. Prudovsky, C. Bagala, F. Tarantini, A. Mandinova, R. Soldi, S. Bellum, T. Maciag, *J. Cell Biol.* **2002**, *158*, 201–208.
- [25] I. Prudovsky, A. Mandinova, R. Soldi, C. Bagala, I. Graziani, M. Landriscina, F. Tarantini, M. Duarte, S. Bellum, H. Doherty, T. Maciag, *J. Cell Sci.* **2003**, *116*, 4871–4881.
- [26] D. Rajalingam, T. K. Kumar, C. Yu, *Biochemistry* **2005**, *44*, 14431–14442.
- [27] J. Vazquez, J. Tautz, J. J. Ryan, K. Vuori, T. Mustelin, M. Pellecchia, *J. Med. Chem.* **2007**, *50*, 2137–2143.
- [28] S. Vanwetswinkel, R. J. Heetebrij, J. van Duynhoven, J. G. Hollander, D. V. Filippov, P. J. Hajduk, G. Siegal, *Chem. Biol.* **2005**, *12*, 207–216.
- [29] T. Marquardsen, M. Hofmann, J. G. Hollander, C. M. Loch, S. R. Kiihne, F. Engelke, G. Siegal, *J. Magn. Reson.* **2006**, *182*, 55–65.
- [30] W. Jahnke, A. Florsheimer, M. J. Blommers, C. G. Paris, J. Heim, C. M. Nalin, L. B. Perez, *Curr. Top. Med. Chem.* **2003**, *3*, 69–80.
- [31] W. Jahnke, H. Widmer, *Cell. Mol. Life Sci.* **2004**, *61*, 580–599.
- [32] X. Salvatella, E. Giral, *Chem. Soc. Rev.* **2003**, *32*, 365–372.
- [33] C. Dalvit, G. Fogliatto, A. Stewart, M. Veronesi, B. Stockman, *J. Biomol. NMR* **2001**, *21*, 349–359.
- [34] Y. Oyama, T. Shishibori, K. Yamashita, T. Naya, S. Nakagiri, H. Maeta, R. Kobayashi, *Biochem. Biophys. Res. Commun.* **1997**, *240*, 341–347.
- [35] T. Shishibori, Y. Oyama, O. Matsushita, K. Yamashita, H. Furuichi, A. Okabe, H. Maeta, Y. Hata, R. Kobayashi, *Biochem. J.* **1999**, *338*, 583–589.
- [36] A. L. Hopkins, C. R. Groom, A. Alex, *Drug Discovery Today* **2004**, *9*, 430–431.
- [37] I. D. Kuntz, K. Chen, K. A. Sharp, P. A. Kollman, *Proc. Natl. Acad. Sci. USA* **1999**, *96*, 9997–10002.
- [38] R. A. Carr, M. Congreve, C. W. Murray, D. C. Rees, *Drug Discovery Today* **2005**, *10*, 987–992.
- [39] K. A. Mercier, M. Baran, V. Ramanathan, P. Revesz, R. Xiao, G. T. Montellione, R. Powers, *J. Am. Chem. Soc.* **2006**, *128*, 15292–15299.
- [40] Y. Oyama, T. Shishibori, K. Yamashita, T. Naya, S. Nakagiri, H. Maeta, R. Kobayashi, *Biochem. Biophys. Res. Commun.* **1997**, *240*, 341–347.
- [41] T. Shishibori, Y. Oyama, O. Matsushita, K. Yamashita, H. Furuichi, A. Okabe, H. Maeta, Y. Hata, R. Kobayashi, *Biochem. J.* **1999**, *338*, 583–589.
- [42] P. J. Hajduk, J. R. Huth, S. W. Fesik, *J. Med. Chem.* **2005**, *48*, 2518–2525.
- [43] M. Assfalg, I. Bertini, R. Del Conte, A. Giachetti, P. Turano, *Biochemistry* **2007**, *46*, 6232–6238.
- [44] F. Arnesano, L. Banci, I. Bertini, A. Fantoni, L. Tenori, M. S. Viezzoli, *Angew. Chem.* **2005**, *117*, 6499–6502; *Angew. Chem. Int. Ed.* **2005**, *44*, 6341–6344.
- [45] P. M. Kilby, L. J. Van Eldik, G. C. Roberts, *FEBS Lett.* **1995**, *363*, 90–96.
- [46] S. Grzesiek, A. Bax, G. M. Clore, A. M. Gronenborn, J. S. Hu, J. Kaufman, I. Palmer, S. J. Stahl, P. T. Wingfield, *Nat. Struct. Biol.* **1996**, *3*, 340–345.

Received: April 27, 2007

Revised: July 3, 2007

Published online on August 20, 2007